Microchimica Acta (2018) 185: 144
https://doi.org/10.1007/s00604-018-2683-z

ORIGINAL PAPER

Aptamer based fluorometric determination of ATP by exploiting the FRET between carbon dots and graphene oxide

Xia Cheng[1] · Yao Cen[1] · Guanhong Xu[1] · Fangdi Wei[1] · Menglan Shi[1] · Xiaoman Xu[1] · Muhammad Sohail[1] · Qin Hu[1]

Received: 8 November 2017 / Accepted: 15 January 2018 / Published online: 29 January 2018

Abstract

The authors describe a fluorometric aptamer based assay for adenosine triphosphate (ATP). It is based on the use of carbon dots (CDs) and graphene oxide (GO). The resultant CD-aptamer is adsorbed on the surface of GO via π-stacking and hydrophobic interaction, and the fluorescence of CD-aptamer is quenched via fluorescence resonance energy transfer (FRET) between CDs and GO. If ATP is present, it will bind to the aptamer and the CD-aptamer will be desorbed from GO. This will suppress FRET and the fluorescence of the CDs is restored. Under the optimal conditions and at typical excitation/emission wavelengths of 358/455 nm, the assay has a 80 pM detection limit and a linear range that extends from 0.10 to 5.0 nM concentrations of ATP. The method was successfully applied to the determination of ATP in yogurt samples. This method can also be conceivably applied to the detection of other analytes for which appropriate aptamers are available.

Keywords Fluorescence · Aptamer · Carbon dots · Adenosine triphosphate · Yogurt · Fluorescence resonance energy transfer · Dairy product · Food safety · Food analysis · Quenching

Introduction

Adenosine triphosphate (ATP) is a general energy source and also used as a mediator of extracellular signalling [1, 2]. By monitoring the content of ATP, one can obtain information on the development of various diseases such as ischemia, cardiovascular disease, hypoglycemia and some malignancies [3]. In addition, ATP is also used as an indicator of food safety as well as environmental analysis. Therefore, developing a rapid, economical, highly sensitive and selective method for detection of ATP is of great importance. Several ATP assays have been developed, including electrochemical biosensor [4], mass spectrometry [5], and aptamer-based methods [6–8]. Among the above assays, the aptamer-based methods are attractive due to their sensitivity, selectivity and low cost.

Fluorometry has become popular in biochemistry and medicine due to the merits of high sensitivity and simplicity [9]. Among various fluorescent materials, the emerging CDs have attracted tremendous attentions owing to their superiorities including low toxicity, excellent photostability, low cost, and convenience in surface functionalization [10].

To improve the selectivity of fluorescent assay, aptamers are introduced. Aptamers are single stranded DNA or RNA molecules selected in vitro through systematic evolution of ligand by exponential enrichment (SELEX). They exhibit high affinity to specific targets such as small molecules, virus, protein, amino acid and cells based on the adaptive recognition involving conformational alteration [11, 12]. Due to the advantages of small size, facile modification, chemical stability, high selectivity and low-cost, aptamers have gained increasing interest [13, 14].

Generally, a fluorometric assay based on fluorescence resonance energy transfer (FRET) usually comprises of a fluorophore and a quencher molecule. To date, many nanomaterials are employed as efficient fluorescence quenchers, especially for GO, which exhibits very high quenching efficiency as well as good repeatability [15]. GO is an interesting nanomaterial with single atom thick, two dimensional graphitic carbon system. Also it has various oxygen-containing functional groups on the surface such as carboxyl, hydroxyl and epoxy group [16]. The huge conjugate structure of GO makes it as an efficient

Electronic supplementary material The online version of this article (https://doi.org/10.1007/s00604-018-2683-z) contains supplementary material, which is available to authorized users.

✉ Qin Hu
huqin@njmu.edu.cn

[1] School of pharmacy, Nanjing medical university, Nanjing, Jiangsu 211166, People's Republic of China

fluorescence quencher based on the photo-induced electron transfer mechanism or energy transfer mechanism [17, 18]. Therefore, the fluorescent labeled single stranded oligonucleotides can be adsorbed on the surface of GO through hydrophobic and π stacking interactions [19], and then the fluorescence of carbon dots can be quenched via FRET. Moreover, as a carbon skeleton material, GO possesses low cytotoxicity, superior fluorescence quenching and adsorption capacity. At present, it has been increasingly applied in making FRET biosensors, aptasensors, drug-delivery vehicles and imaging agents [20, 21]. To our knowledge, a fluorometric assay based on FRET between CDs and GO for ATP detection has not been reported.

Here we describe a novel fluorometric ATP assay by using aptamer labeled CDs and GO. The CDs possessing strong fluorescence were synthesized through a hydrothermal method, and the aptamer was modified on the surface of CDs. CD-aptamer complex acted as the energy donor and molecular recognition probe. It can be adsorbed onto GO which served as the FRET acceptor through π stacking and hydrophobic interactions. Then the fluorescence of CDs was turned off. When ATP was present, it combined with the aptamer selectively and CD-aptamer was released from GO. Subsequently, the FRET process was blocked and the fluorescence of CDs recovered. The assay had very high sensitivity and selectivity for detecting ATP. Finally, the platform was successfully applied to the determination of ATP in yogurt.

Materials and methods

Reagents and materials

N-(3-Dimethylaminopropyl)-N-ethylcarbodiimide hydrochloride (EDC), citric acid monohydrate, N-hydroxysuccinimide (NHS), glucose (Glu), ascorbic acid (AA), galactose (Gal), sodium hydroxide, ferric chloride hexahydrate ($FeCl_3·6H_2O$) were purchased from Sinopharm Chemical Reagent Co., Ltd. (Shanghai, China, http://www.sinoreagent.com/). Diethylene triamine, acetone, disodium hydrogen phosphate, and sodium dihydrogen phosphate were purchased from Shanghai Lingfeng Chemical Reagent Co., Ltd. (Shanghai, China, http://lingfenghx.cn.makepolo.com/). GO was purchased from Suzhou Tanfeng Graphene Tech Co., Ltd. (Suzhou, China, http://graphenechina.cnpowder.com.cn/). ATP, uridine triphosphate (UTP), guanosine triphosphate (GTP), and cytidine triphosphate (CTP) were purchased from Aladdin Chemistry Co., Ltd. (Shanghai, China, http://www.aladdin-e.com/). The purified water used in the study was prepared by Direct-Q water purification system (Millipore, USA, http://millipore.bioon.com.cn/). Phosphate buffered saline containing 0.9% NaCl was prepared by the mixing stock solution of $Na_2HPO_4·12H_2O$ and $NaH_2PO_4·2H_2O$. All reagents were of analytical grade and without any further purification. ATP aptamer was purchased from Shanghai Sangon Biological Engineering Technology & Services Co., Ltd. (Shanghai, China, http://www.sangon.com/) and its base sequence is given as follows: 5′-NH_2-$(CH_2)_6$-ACC TGG GGG AGT ATT GCG GAG GAA GGT-3′.

Apparatus

Fourier-transform infrared spectra were recorded on a TENSOR 27 spectrometer (Bruker, Germany, https://www.bruker.com/) with a resolution of 2 cm^{-1} and a spectral range of 4000–400 cm^{-1} using pelletizing a homogenized powder of the synthesized nanoparticles and KBr. The fluorescence spectra were measured with an F-4600 fluorescence spectrophotometer (Hitachi, Japan, http://www.hitachi.com/). UV-vis absorption spectra were acquired on a UV2450 spectrometer (Shimadzu, Japan, https://www.shimadzu.com.cn/). The transmission electron microscopic (TEM) and high-resolution transmission electron microscopic (HRTEM) images were recorded with a JEOL JEM-2100 (HR) transmission electron microscopy (Tokyo, Japan, https://www.jeol.co.jp/en/products/detail/JEM-2100F.html). Raman signals were collected by Thermo Fisher DXR Raman Microscope (Madison, USA, http://www.thermofisher.com/). The combination between aptamer and CDs was confirmed by agarose gel electrophoresis (Shanghai Tanon HE-120, http://www.biotanon.com/) in 6.0% agarose gel with 0.5 × TBE buffer at 100 V for 1 h.

Preparation of CDs

CDs were synthesized according to a reported method [22]. In summary, 1.2 g of citric acid monohydrate and 600 μL of diethylene triamine were dissolved in 20 mL of ultrapure water. Then the mixture was transferred to a Teflon equipped stainless steel autoclave (30 mL) and followed by hydrothermal treatment at 200 °C for 4 h. When cooled down to room temperature, the products were concentrated by rotary evaporation, followed by purification with acetone for three times. The final products were dispersed in ultrapure water as stock solution (8 μg mL^{-1}) after vacuum drying overnight.

Synthesis of CD-aptamer conjugates

Amino-modified ATP aptamers were dissolved in PBS (pH 7.4). Immobilization was carried out by the well-established carbodiimide chemistry [23]. Specifically, 500 μL of 0.1 M EDC/NHS in 10 mM PBS was added to 250 μL of CDs solution and the mixture was sonicated for 30 min. Then the pH value of the solution was adjusted to 7.5 by 0.1 M NaOH. After that, 250 μL of 60 μM ATP aptamer in 10 mM PBS was added to the mixture, and further incubated for 12 h at 25 °C. The final products were stored at 4 °C.

Determination of ATP

The determination of ATP was conducted as follows: 50 μL of GO solution (0.1 mg mL^{-1}) was added to 100 μL of CD-aptamer solution, and then the mixture was incubated at 25 °C for 20 min. Afterwards, 50 μL of different concentrations of ATP standard solutions were added into the mixture and incubated at 25 °C for 40 min with the help of a reciprocating oscillator. The signal output values were calculated according to the relative fluorescence intensity [$(F-F_0)/F_0$], in which F and F_0 represent the fluorescence of the system in the presence and absence of ATP (λ_{exc} = 358 nm and λ_{em} = 455 nm), respectively.

Preparation of yogurt samples

The fresh yogurt samples which contained lactobacillus bulgaricus, streptococcus thermophilus, lactobacillus acidophilus, bifidobacterium lactis, lactobacillus casei were purchased from a local supermarket and the storage temperature was 2 –6 °C. Sample 1 was stored in the refrigerator at 4 °C while sample 2 was kept at room temperature overnight. The samples were prepared according to a reported method with a little modification [24]. First, 100 μL of yogurt was diluted to 1 mL, and the mixture was centrifuged at 12000 rpm for 10 min. Then the supernatant was removed and 1 mL of boiling saline buffer was added in the sediment. After that, the solution was kept 100 °C for 10 min, and then the solution was sonicated while it was hot. After 10 min, the solution was centrifuged at 12000 rpm for 10 min and the supernatant was diluted 100-fold using buffer). Finally, the diluted yogurt samples spiked with different concentrations of ATP were detected as described in Determination of ATP.

Results and discussion

The principle of ATP assay

As demonstrated in Scheme 1, the aptamer of ATP is modified on the surface of CDs according to the carbodiimide chemistry. When GO is introduced into the system, CD-aptamer can be adsorbed on the surface of GO through π stacking and hydrophobic interactions. As a result, it brings the CD-aptamer in close proximity to GO (<10 nm) [19]. According to the experimental results shown in Fig. 1 (A), GO has a broad absorption from 200 to 800 nm. The fluorescence emission spectrum of CD-aptamer overlaps with the absorption spectrum of GO. CD-aptamer can act as the energy donor and molecular recognition probe, and GO can serve as energy acceptor. So, FRET between CD-aptamer and GO happens when they get close to each other, and the fluorescence of CD-aptamer is quenched. In the presence of ATP, it can bind with the aptamer with high affinity and specificity. Then the globular chain structures are formed on the surface of CDs, and CD-aptamer is released from GO. Consequently, the fluorescence of CD-aptamer recovers, which can be seen in Fig. 1 (B).

To further investigate the mechanism of fluorescence quenching, we measured the Stern-Volmer quenching constants based on CD-aptamer versus concentration of GO at three different temperatures (288, 298, and 310 K). The Stern-Volmer equation is described as $F_0/F = 1 + K_{sv}C$ (C is the concentration of quencher, K_{sv} is the Stern-Volmer quenching constants, F_0 and F are the fluorescence intensity of the fluorophore without quencher and with different concentrations of quencher, respectively). It is reported that K_{sv} will decrease with rising temperature in static quenching and the reverse in dynamic quenching [25]. According to Fig. S1,

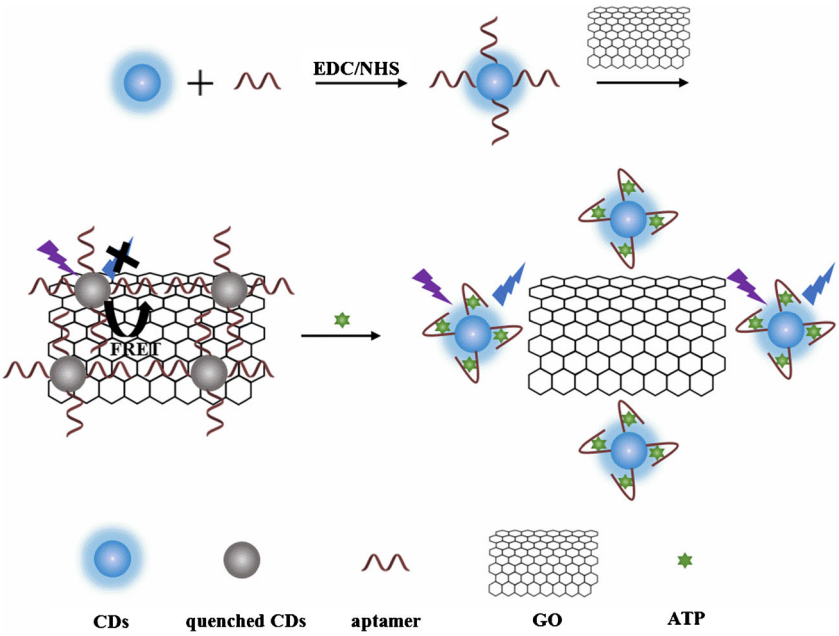

Scheme 1 Schematic illustration of the assay based on the FRET between CDs and GO for ATP detection

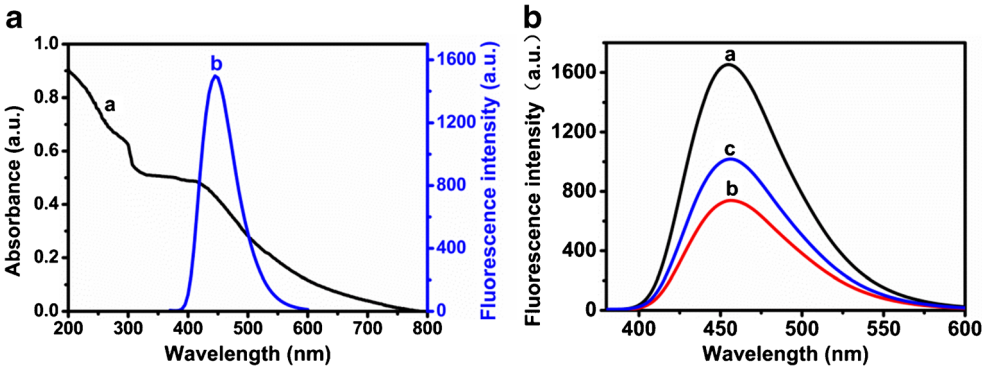

Fig. 1 **a** UV-vis absorption spectrum of GO (a) and fluorescence emission spectrum of CD-aptamer (b). **b** Fluorescence emission spectra of CD-aptamer (a), CD-aptamer/GO (b) and CD-aptamer/GO with the addition of ATP (c)

K_{sv} is inversely proportional to the temperature. It reveals that the CD-aptamer/GO system is a static quenching process.

Characterization of CDs

To verify the morphology and structure of CDs, TEM, UV-vis absorption spectra, fluorescence spectra, FT-IR spectra and Raman spectra were performed. In Fig. 2A, the typical TEM image shows that the CDs are spherical, well-dispersed and exhibit a narrow size distribution of 1.5–3.0 nm. The inset in Fig. 2A shows that the lattice spacing of the CDs is 0.22 nm, which is similar than that of other previous reported CDs [26].

As shown in Fig. 2B, CDs have two absorption peaks at 240 nm and 358 nm. The peak at 240 nm is originated from the π–π* transition of the aromatic ring structure and the peak at 358 nm is attributed to the n-π* transition of the -C=O group [27]. The maximum excitation and the maximum emission wavelength of the CDs are recorded to be 358 nm and 446 nm, respectively. The aqueous solution of CDs exhibits colorless under visible light while emits blue luminescence under 365 nm UV illumination (inset of Fig. 2B).

The FT-IR spectrum of CDs is displayed in Fig. 2C. The absorption peak at 3413 cm^{-1} is attributed to -OH and the characteristic peak centered at 1654 cm^{-1} corresponds to the stretching vibration of -C=O. The obvious peaks at 3246 cm^{-1} and 1550 cm^{-1} are attributed to the stretching vibration and bending vibration of -NH, respectively. In addition, the peak at 2897 cm^{-1} is assigned to the stretching vibration of C-H. The results indicate that there are plenty of carboxy and amino groups on the surface of the CDs.

Figure 2D depicts the optical stability of CDs. CDs are excited at the maximum excitation wavelength for 2 h. The fluorescence intensity of the CDs has no obvious change. It indicates that CDs possess good resistance to photobleaching.

The Raman spectra (Fig. S2) show that the CDs have the characteristic peaks at 1454 and 1736 cm^{-1}, which are similar with GO. The peak at 1454 cm^{-1} (D band) is due to the presence of carbon atoms of disordered graphite, and the peak at 1736 cm^{-1} (G band) is attributed to the C-C bond

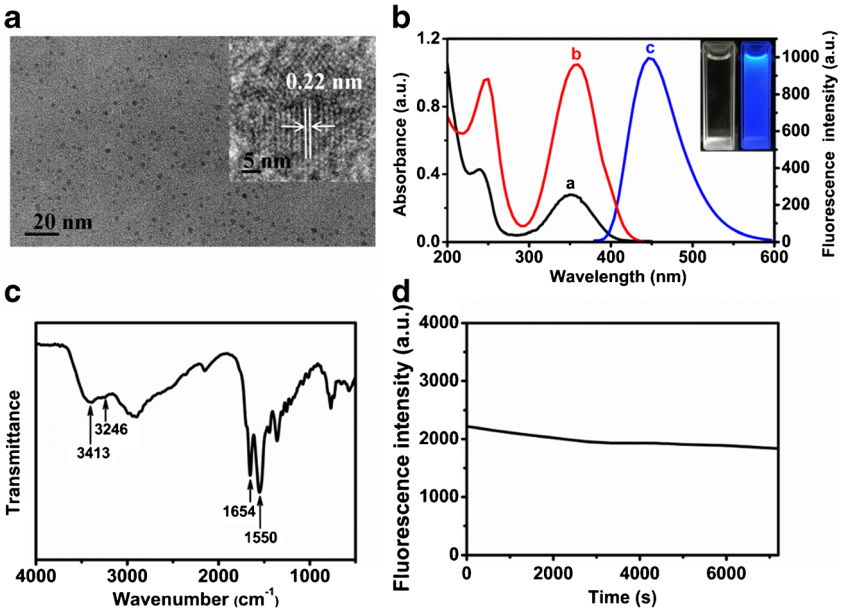

Fig. 2 Characterizations of CDs: **a** TEM images; Inset: High-resolution TEM image. **b** UV-vis absorption spectrum (a), fluorescence excitation (b), and emission spectrum (c); Inset shows the photographs of prepared CDs in PBS under visible light (left) and 365 nm UV lamp light (right). **c** FT-IR spectrum. **d** Fluorescence emission spectrum of CDs excited at 358 nm for 2 h

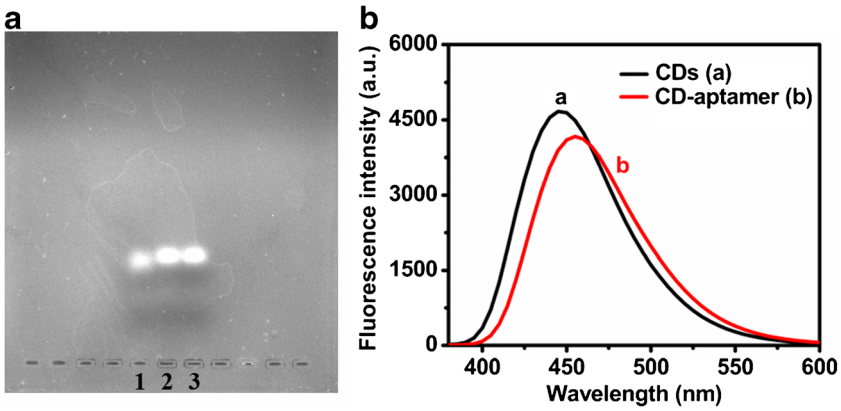

Fig. 3 **a** Agarose gel electrophoresis of aptamer modified CDs. Lane 1: CD-aptamer, Lane 2: aptamer, Lane 3: the mixture of aptamer and CDs. **B** Fluorescence spectra of CDs (a) and CD-aptamer (b)

stretching vibrations [28]. The results confirm that the CDs are carbon based materials as same as GO.

Characterization of GO

TEM image and Raman spectrum of GO are shown in Fig. S3 and Fig. S2, respectively. The TEM image emphasizes the flake-like shape of the material. The Raman spectrum of GO displays a D-band at 1278 cm^{-1} and a G-band at 1617 cm^{-1}, in agreement with the literature [29]. The D-band at 1278 cm^{-1} is ascribe to the vibrations of disordered/oxidized carbons at edges and the defect sidewalls, and the G-band at 1617 cm^{-1} assigns to the vibrations of graphitic carbons [30].

Characterization of CD-aptamer

To demonstrate the successful modification of ATP aptamer on the surface of the CDs, the agarose gel electrophoresis and fluorescence spectrum were performed. Figure 3A shows that CD-aptamer moves slower than the plain aptamer and the mixture of CDs and aptamer, which is owing to the increase of mass-to-charge ratio of CD-aptamer than the plain aptamer [31]. As shown in Fig. 3B, the emission peak of CD-aptamer exhibits a red shift from 446 nm to 455 nm compared with the peak of CDs (λ_{ex} = 358 nm). This is mainly due to the covalent binding of aptamer to the CDs surface, which changes the surface charge of CDs [32] and the size of CDs [33]. Both agarose gel electrophoresis and fluorescence spectrum prove that the aptamer is successfully modified on the surface of the CDs.

Optimization of experimental conditions

The following parameters are optimized: (A) pH value of the system, (B) the concentrations of aptamer and GO, (C) incubation time, (D) incubation temperature.

Respective experimental data and figures are given in Fig. S4. The following experimental conditions were found to give best results: (A) pH 7.4; (B) the concentration of aptamer: 15 μM, and the concentration of GO: 0.1 mg mL^{-1}; (C) incubation time of the CD-aptamer/GO reacting with ATP: 40 min, (D) incubation temperature for the CD-aptamer/GO reacting with ATP and the conjunction between CDs and aptamer: 25 °C.

Selectivity and interference

To validate the selectivity of the assay for the determination of ATP, three ATP analogues including UTP, CTP, and GTP were evaluated. As shown in Fig. 4A, there is a significant increase of fluorescence signal for single ATP at a concentration of 3 nM and the mixture of ATP (3 nM), UTP (1 μM), CTP (1 μM) and GTP (1 μM) respectively, while the fluorescence signals for 1 μM of UTP, CTP and GTP, respectively, are neglectable. This result indicates that the assay possesses high

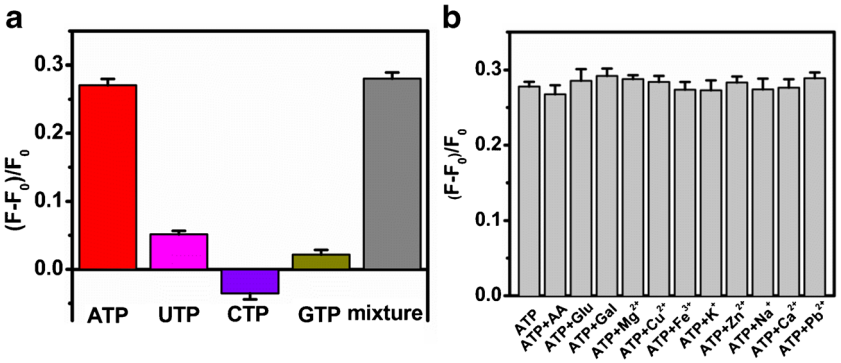

Fig. 4 **a** Responses of the assay to ATP (3 nM), other analogues (1 μM) and the mixture of ATP, UTP, CTP and GTP. **b** Fluorescence intensity change of the assay to ATP (3 nM) in the absence and presence of other potential interferents: AA (1 μM), Glu (1 μM), Gal (1 μM), Mg^{2+} (0.2 μM), Cu^{2+} (0.1 μM), Fe^{3+} (0.1 μM), K^{+} (1 μM), Zn^{2+} (1 μM), Na^{+} (1 μM), Ca^{2+} (1 μM), Pb^{2+} (1 μM)

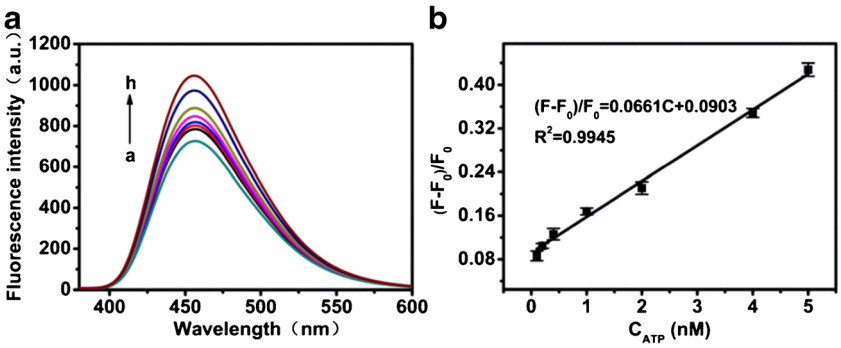

Fig. 5 **a** Fluorescence emission spectra (λ_{ex} = 358 nm and λ_{em} = 455 nm) of CD-aptamer/GO assay in the presence of different concentrations of ATP (from a to h: 0, 0.10, 0.20, 0.40, 1.0, 2.0, 4.0, 5.0 nM). **b** Calibration curve: fluorescence intensity changes [$(F–F_0)/F_0$] versus the concentration of ATP (0.10–5.0 nM)

selectivity due to the high affinity of ATP with its aptamer. At the same time, various ions and molecules as interferences, including AA, Glu, Gal, Mg^{2+}, Cu^{2+}, Fe^{3+}, K^+, Zn^{2+}, Na^+, Ca^{2+}, Pb^{2+} were evaluated (Fig. 4B). The result shows that the fluorescence intensity has no obvious change when ATP is mixed with other interferents compared with ATP alone.

Method validation

Under optimized conditions, the fluorescence intensity at excitation/emission wavelengths of 358/455 nm of the system increases linearly with the increase of ATP in the range of 0.10 nM to 5.0 nM, as shown in Fig. 5. The linear equation can be expressed as $(F\text{-}F_0)/F_0 = 0.0661c + 0.0903$ (where F and F_0 are the fluorescence intensity of ATP detection system in the presence and absence of ATP, respectively, c represents the concentration of ATP, nM) with the correlation coefficient of $R^2 = 0.9945$, and the limit of detection (LOD) for ATP was 80 pM based on 3σ/K (σ is the standard deviation of blank measurements ($n = 10$), and K is the slope of calibration graph). Table S1 lists the limit of detection and dynamic range obtained by this work and reported methods. As can be seen from Table S1, compared with other methods reported previously, the LOD of our method is lower or comparable than those of other methods reported and it obtains good sensitivity. As shown in Table 1, the intra-day and the inter-day relative standard deviations (RSDs) of this method are all less than 10%. The result suggests that the method possesses good reproducibility.

Analytical application in real sample

To evaluate the feasibility of the method, the assay was applied to the determination of ATP in yogurt samples by using the standard addition method. The analytical results are summarized in Table 2. It can be seen that the recoveries of ATP added in the real samples are in the range of 90.0–110% with RSDs less than 10%. The results indicate that the precision and accuracy of the method meet the needs of biological sample analysis. Furthermore, we found that the concentration of ATP in sample 2 stored at 25 °C was higher than that stored at 4 °C, which coincided with the fact that 0–4 °C inhibits the activities of some microorganisms, while the high temperature promotes the growth of various kinds of bacteria, which lead to the increase of ATP [34, 35].

Conclusion

In summary, a novel fluorescence assay based on fluorescence resonance energy transfer is successfully established for sensitive and selective determination of ATP. The fluorescence of CD-aptamer is quenched by GO via FRET and is further recovered owing to the strong affinity between ATP and the aptamer in the presence of ATP. In addition, the assay exhibits several advantages compared to previous methods: (1) All materials used in the assay are cheap, available and eco-friendly. (2) The assay shows good sensitivity and selectivity compared with other ATP assays using FRET or other

Table 1 The intra-day and inter-day precisions of the determination of ATP ($n = 3$)

Concentration of ATP (nM)	intra-day (nM)	RSD (%)	inter-day (nM)	RSD (%)
0.20	0.22	4.4	0.22	7.1
	0.23		0.20	
	0.24		0.23	
1.00	1.06	2.4	1.06	8.5
	1.01		0.97	
	1.04		1.15	
4.00	3.93	2.1	3.93	3.0
	3.80		3.88	
	3.95		3.71	

Table 2 Determination of ATP in yogurt samples (n = 3)

Sample	Spiked (nM)	Found (nM)	Recovery (%)	RSD (%)
1	0	0.55	–	7.9
	0.80	1.40	106.5	2.9
	1.60	2.15	99.7	4.2
	2.40	2.97	100.9	3.3
2	0	0.97	–	6.5
	0.80	1.74	96.3	2.3
	1.60	2.58	100.6	8.3
	2.40	3.25	95.0	2.7

techniques. Furthermore, the platform is successfully applied to the determination of ATP in yogurt samples. Considering this, the system holds great potential for monitoring the food safety as well as environmental pollution.

Acknowledgements This work was financially supported by the National Natural Science Foundation of China (No. 61775099, No. 21705080), the Natural Science Foundation of Jiangsu Province (No. BK20171487, No. BK20171043), and the Natural Science Foundation of the Higher Education Institutions of Jiangsu Province (No. 17KJB150029).

Compliance with ethical standards The author(s) declare that they have no competing interests.

References

1. Wang J, Jiang Y, Zhou C, Fang X (2005) Aptamer-based ATP assay using a luminescent light switching complex. Anal Chem 77:3542–3546. https://doi.org/10.1021/ac050165w
2. Zeng X, Zhang X, Yang W, Jia H, Li Y (2012) Fluorescence detection of adenosine triphosphate through an aptamer-molecular beacon multiple probe. Anal Biochem 424:8–11. https://doi.org/10.1016/j.ab.2012.01.021
3. Ma C, Yang X, Wang K, Tang Z, Li W, Tan W, Lv X (2008) A novel kinase-based ATP assay using molecular beacon. Anal Biochem 372:131–133. https://doi.org/10.1016/j.ab.2007.08.003
4. Tang DP, Hou L (2016) Aptasensor for ATP based on analyte-induced dissociation of ferrocene-aptamer conjugates from manganese dioxide nanosheets on a screen-printed carbon electrode. Microchim Acta 183:2705–2711. https://doi.org/10.1007/s00604-016-1916-2
5. Kennedy HJ, Pouli AE, Ainscow EK, Jouaville LS, Rizzuto R, Rutter GA (1999) Glucose generates sub-plasma membrane ATP microdomains in single islet β-cells: potential role for strategically located mitochondria. J Biol Chem 274:13281–13291. https://doi.org/10.1074/jbc.274.19.13281
6. Chen Z, Li G, Zhang L, Jiang JF, Li Z, Peng ZH, Deng L (2008) A new method for the detection of ATP using a quantum-dot-tagged aptamer. Anal Bioanal Chem 392:1185–1188. https://doi.org/10.1007/s00216-008-2342-z
7. Gao PY, Xia YF, Yang LL, Ma TF, Yang L, Guo QQ, Huang SS (2014) Aptasensor for adenosine triphosphate based on electrode-supported lipid bilayer membrane. Microchim Acta 181:205–212. https://doi.org/10.1007/s00604-013-1100-x
8. Zhang SS, Yan YM, Bi S (2009) Design of molecular beacons as signaling probes for adenosine triphosphate detection in cancer cells based on chemiluminescence resonance energy transfer. Anal Chem 81:8695–8701. https://doi.org/10.1021/ac901759g
9. Cui ZQ, Ren Q, Wei HP, Chen Z, Deng JY, Zhang ZP, Zhang XE (2011) Quantum dot-aptamer nanoprobes for recognizing and labeling influenza a virus particles. Nano 3:2454–2457. https://doi.org/10.1039/c1nr10218d
10. Lim SY, Shen W, Gao ZQ (2015) Carbon quantum dots and their applications. Chem Soc Rev 44:362–381. https://doi.org/10.1039/C4CS00269E
11. Citartan M, Gopinath SCB, Tominaga J, Tan SC, Tang TH (2012) Assays for aptamer-based platforms. Biosens bioelectron 34:1–11. https://doi.org/10.1016/j.bios.2012.01.002
12. Pilehvar S, Mehta J, Dardenne F, Robbens J, Blust R, De Wael K (2012) Aptasensing of chloramphenicol in the presence of its analogues: reaching the maximum residue limit. Anal Chem 84:6753–6758. https://doi.org/10.1021/ac3012522
13. Feng CJ, Dai S, Wang L (2014) Optical aptasensors for quantitative detection of small biomolecules: a review. Biosens Bioelectron 59:64–74. https://doi.org/10.1016/j.bios.2014.03.014
14. Chiu TC, Huang CC (2009) Aptamer-functionalized nano-biosensors. Sensors 9:10356–10388. https://doi.org/10.3390/s91210356
15. Zhang H, Zhang HL, Aldalbahi A, Zuo XL, Fan CH, Mi XQ (2017) Fluorescent biosensors enabled by graphene and graphene oxide. Biosens Bioelectron 89:96–106. https://doi.org/10.1016/j.bios.2016.07.030
16. Liu MC, Chen CL, Hu J, Wu XL, Wang X (2011) Synthesis of magnetite/graphene oxide composite and application for cobalt(II) removal. Phys Chem C 115:25234–25240. https://doi.org/10.1021/jp208575m
17. Loh KP, Bao Q, Eda G, Chhowalla M (2010) Graphene oxide as a chemically tunable platform for optical applications. Nat Chem 2:1015–1024. https://doi.org/10.1038/NCHEM.907
18. Zhang C, Yuan Y, Zhang S, Wang Y, Liu Z (2011) Biosensing platform based on fluorescence resonance energy transfer from upconverting nanocrystals to graphene oxide. Angew Chem Int Ed 50:6851–6854. https://doi.org/10.1002/anie.201100769
19. Wu M, Kempaiah R, Huang PJJ, Maheshwari V, Liu JW (2011) Adsorption and desorption of DNA on graphene oxide studied by fluorescently labeled oligonucleotides. Langmuir 27:2731–2738. https://doi.org/10.1021/la1037926
20. Huang PJJ, Liu J (2012) DNA-length-dependent fluorescence signaling on graphene oxide surface. Small 8:977–983. https://doi.org/10.1002/smll.201102156
21. Lu Z, Chen X, Wang Y, Zheng X, Li CM (2015) Aptamer based fluorescence recovery assay for aflatoxin B1 using a quencher system composed of quantum dots and graphene oxide. Microchim Acta 182:571–578. https://doi.org/10.1007/s00604-014-1360-0
22. Zhu SJ, Meng QN, Wang L, Zhang JH, Song YB, Jin H, Zhang K, Sun HC, Wang HY, Yang B (2013) Highly photoluminescent carbon dots for multicolor patterning, sensors, and bioimaging. Angew Chem 52:3953–3957. https://doi.org/10.1002/anie.201300519
23. Zhang LM, Xia JG, Zhao QH, Liu LW, Zhang ZJ (2010) Functional graphene oxide as a nanocarrier for controlled loading and targeted delivery of mixed anticancer drugs. Small 6:537–544. https://doi.org/10.1002/smll.200901680
24. Yan XL, Chen X, Gao WJ, Wei TT, Lin YM, Ai FR (2017) Nanoparticles grafted by ATP aptamer: preparation and application in Chemiluminescence enzyme analysis. Chinese journal of inorganic chemistry 33:340–346. https://doi.org/10.11862/CJIC.2017.034
25. Zu F, Yan F, Bai Z, Xu J, Wang Y, Huang Y, Zhou X (2017) The quenching of the fluorescence of carbon dots: a review on mechanisms and applications. Microchim Acta 184:1899–1914. https://doi.org/10.1007/s00604-017-2318-9
26. Liu T, Dong JX, Liu SG, Li N, Lin SM, Fan YZ, Lei JL, Luo HQ, Li NB (2017) Carbon quantum dots prepared with polyethyleneimine

as both reducing agent and stabilizer for synthesis of ag/CQDs composite for Hg^{2+} ions detection. J Hazard Mater 322:430–436. https://doi.org/10.1016/j.jhazmat.2016.10.034

27. Feng T, Ai XZ, Ong HM, Zhao YL (2016) Dual-responsive carbon dots for tumor extracellular microenvironment triggered targeting and enhanced anticancer drug delivery. ACS Appl Mater Interfaces 8:18732–18740. https://doi.org/10.1021/acsami.6b06695
28. Zhou J, Zhou H, Tang J, Deng S, Yan F, Li W, Qu M (2017) Carbon dots doped with heteroatoms for fluorescent bioimaging: a review. Microchim Acta 184:343–368. https://doi.org/10.1007/s00604-016-2043-9
29. Kudin KN, Ozbas B, Schniepp HC, Prud'Homme RK, Aksay IA, Car R (2008) Raman spectra of graphite oxide and functionalized graphene sheets. Nano Lett 8:36–41. https://doi.org/10.1021/nl071822y
30. Goud KY, Hayat A, Satyanarayana M, Kumar VS, Catanante G, Gobi KV, Marty JL (2017) Aptamer-based zearalenone assay based on the use of a fluorescein label and a functional graphene oxide as a quencher. Microchim Acta 184:4401–4408. https://doi.org/10.1007/s00604-017-2487-6
31. He SB, Huang BH, Tan JJ, Luo QY, Lin Y, Li J, Hu Y, Zhang L, Yan SH, Zhang Q, Pang DW, Li LJ (2011) One-to-one quantum dot-labeled single long DNA probes. Biomaterials 32:5471–5477. https://doi.org/10.1016/j.biomaterials.2011.04.013
32. Dong HF, Gao WC, Yan F, Ji HX, Ju HX (2010) Fluorescence resonance energy transfer between quantum dots and graphene oxide for sensing biomolecules. Anal Chem 82:5511–5517. https://doi.org/10.1021/ac100852z
33. Liu HY, Xu SM, He ZM, Deng AP, Zhu JJ (2013) Supersandwich Cytosensor for selective and ultrasensitive detection of cancer cells using aptamer-DNA Concatamer-quantum dots probes. Anal Chem 85:3385–3392. https://doi.org/10.1021/ac303789x
34. Snyder AB, Churey JJ, Worobo RW (2016) Characterization and control of Mucor circinelloides spoilage in yogurt. Int J Food Microbiol 228:14–21. https://doi.org/10.1016/j.ijfoodmicro.2016.04.008
35. Hilton ST, de Moraes JO, Moraru CI (2017) Effect of sublethal temperatures on pulsed light inactivation of bacteria. Innovative Food Science and Emerging Technologies 39:49–54. https://doi.org/10.1016/j.ifset.2016.11.002